

Plenary paper

Functional dissection of the chromosome *13q14* tumor-suppressor locus using transgenic mouse lines

Marie Lia,¹ Amanda Carette,² Hongyan Tang,¹ Qiong Shen,¹ Tongwei Mo,¹ Govind Bhagat,^{2,3} Riccardo Dalla-Favera,¹⁻⁵ and Ulf Klein²⁻⁴

¹Institute for Cancer Genetics, ²Herbert Irving Comprehensive Cancer Center, ³Department of Pathology & Cell Biology, ⁴Department of Microbiology & Immunology, and ⁵Department of Genetics & Development, Columbia University, New York, NY

Deletion of chromosomal region *13q14* represents the most common genetic aberration in B-cell chronic lymphocytic leukemia (CLL). *13q14* deletions are commonly large and heterogeneous in size and affect multiple genes. We recently found that targeted deletion in mice of the 0.11 megabase (mb)-long *minimal deleted region (MDR)* encompassing the *DLEU2/miR-15a/16-1* cluster recapitulates the spectrum of CLL-associated lymphoproliferations in humans, including CLL, CD5⁺ monoclonal B-cell lymphocytosis, and CD5⁻ non-Hodgkin lympho-

mas. In the present study, we demonstrate that additional deletion of the 0.69-mb large genomic region telomeric to the *MDR* called the *common deleted region (CDR)* changed the spectrum of lymphoproliferations developing in *CDR*- versus *MDR*-deleted mice in that the number of CLL among B-cell lymphoproliferations was significantly elevated in the former. In addition, *CDR*-deleted mice seemed to succumb to their disease faster than *MDR*-deleted mice. Comparing HCDR3 regions of CD5⁺ lymphoproliferations derived from this and published

CLL mouse models, 44% (29 of 66) of junctions could be assigned to 8 sets of highly similar HCDR3 regions, demonstrating that CLL developing in mice frequently expresses almost identical, stereotypic Ag receptors. These results suggest that the size of *13q14* deletions influences the phenotype of the developing lymphoproliferations and potentially the severity of disease, suggesting a tumor-suppressor function for genetic elements in addition to *DLEU2/miR-15a/16-1*. (*Blood*. 2012;119(13):2981-2990)

Introduction

B-cell chronic lymphocytic leukemia (CLL) is a neoplasm of mature B lymphocytes presenting with an indolent or aggressive disease course. The phenotype of the tumor cells and features of the Ab-binding regions suggest a derivation from Ag-experienced B cells.¹⁻³ CLL is preceded by CD5⁺ monoclonal B-cell lymphocytosis (MBL)^{4,5} and occasionally progresses to diffuse large B-cell lymphoma. CLL is associated with recurrent genomic aberrations including chromosomal gains (trisomy 12) and deletions (*17p*, *11q*, and *13q14*)⁶ and, at a lower frequency, with recurrent somatic mutations in *NOTCH1* and other genes.^{7,8} Deletions of *13q14* are the most common aberration in CLL (55%)^{6,9} and are found at a similar percentage in MBL⁵ and less frequently in diffuse large B-cell lymphoma, multiple myeloma, and several types of non-B cell tumors. The extensive characterization of *13q14* deletions has demonstrated that the break points are heterogeneous and that the deleted region can comprise multiple genes.¹⁰⁻¹⁷ These studies led to the identification of a *minimal deleted region (MDR)*^{12,13} that comprises the *deleted in leukemia 2 (DLEU2)* gene encoding a sterile RNA transcript and the microRNA 15a/16-1 cluster¹⁸ that is located in an intron of *DLEU2* (Figure 1); this *DLEU2/miR-15a/16-1* locus is invariably affected by deletions in all CLL with *13q14* aberrations. Functional evidence has long suggested an involvement of *miR-15a/16-1* deletion in CLL development,¹⁹⁻²¹ and the causative role of *miR-15a/16-1* in CLL pathogenesis has been demonstrated recently in vivo in a knockout mouse model in which these microRNAs were specifically deleted in B cells.²² This same

study also demonstrated that a larger deletion (*MDR*) affecting the host gene of these microRNAs, *dleu2*, as well as the *dleu5* and *kcnrg* genes (that in the mouse overlap with the *dleu2/miR-15a/16-1* locus), shows a significantly more aggressive disease course.²² These results therefore suggest that additional genetic elements within the *13q14* locus in addition to *miR-15a/16-1* may act as tumor suppressors, and that their concomitant deletion with *miR-15a/16-1* may exacerbate the disease course.

Whereas the analysis of the *MDR* has led to the definition of the minimal targets of the *13q14* deletion, it must be noted that the deletions are usually significantly larger in CLL. In particular, a 0.9-megabase (mb) region telomeric to the *DLEU2/miR-15a/16-1* cluster is frequently deleted in combination with the *MDR* and is therefore referred to as the *common deleted region (CDR)* (Figure 1). The deleted region telomeric to *DLEU2/miR-15a/16-1* comprises 3 genes, namely *DLEU1*, *DLEU7*, and *RNASEH2B* (Figure 1), of which only the latter 2 genes are conserved across species. *DLEU1* encodes a sterile transcript of unknown function and, because of its lack of evolutionary conservation, has not been considered a candidate tumor-suppressor gene. Functional studies of *DLEU7*, a protein-encoding gene,²³ in non-B cells suggest that it may act as an inhibitor of several signaling pathways that promote cell-cycle entry.²⁴ In the majority of CLL cases analyzed, *DLEU7* expression was low and associated with promoter methylation.²³ It is presently unclear whether *DLEU7* is methylated specifically in CLL and to what extent promoter methylation plays a role in CLL

Submitted September 27, 2011; accepted December 2, 2011. Prepublished online as *Blood* First Edition paper, December 15, 2011; DOI 10.1182/blood-2011-09-381814.

There is an *Inside Blood* commentary on this article in this issue.

The online version of this article contains a data supplement.

© 2012 by The American Society of Hematology

pathogenesis. Mutations in *RNASEH2B* (*AGS2/DLEU8/FLJ11712*), which encodes the ribonuclease H2 subunit B that is involved in eliminating RNA-DNA intermediates during replication, are associated with Aicardi-Goutières syndrome,²⁵ a rare recessive neurologic disorder. The expression pattern and function of *RNASEH2B* in B cells is unknown.

The present study is a continuation of our efforts to elucidate the tumor-suppressor function of the *13q14* locus that shows extensive heterogeneity in the sizes of the deleted regions. We constructed a *CDR* conditional knockout mouse that, in addition to the *h13q14/m14qC3 MDR*,²² has the genomic region telomeric to the *MDR* deleted. We sought to determine whether the loss of genes in the *h13q14/m14qC3* locus in addition to those encoded in the *MDR* change the spectrum of lymphoproliferations and/or the disease course. We also compared the rearranged Ig heavy chain–variable region genes of the CD5⁺ B-cell lymphoproliferations developing in the *CDR*-deleted mice with those observed in *miR-15a/16-1, MDR*-deleted,²² and *TCL1-Tg* mice²⁶ to determine whether similar to human CLL, independent CLL mouse models are characterized by the expression of highly identical, stereotypic Ag receptors.

Methods

Generation of *CDR*-conditional and *CDR*-null mice

The 2 targeting vectors used to flank the *CDR* with *loxP* and *frt* sites were derivatives of pEmod2²⁷ containing either a phosphoglycerate kinase (PK)–neomycin-resistance (5′ tag) or a PK–hygromycin-resistance (3′ tag) poly(A) cassette, the herpes simplex virus thymidine kinase gene (both tags), a *loxP* and a *frt* site (both tags), a promoterless gene encoding enhanced green fluorescent protein (eGFP) and immediately preceding a triple simian virus 40 poly(A) site in 5′ tag, a PK promoter (3′ tag), and multiple unique restriction sites for cloning 14qC3 segments corresponding to the homology arms (supplemental Figure 1-A1 and A2, available on the *Blood* Web site; see the Supplemental Materials link at the top of the online article). The vectors were constructed so that in the appropriate cell type, Flp-mediated recombination produced deletion of the whole targeted region (supplemental Figure 1-A3) and Cre-mediated recombination produced deletion of the *CDR* with simultaneous activation of eGFP expression (supplemental Figure 1-A4). Successively inserted into the cloning sites of the corresponding 5′ tag and 3′ tag vectors were 2 DNA fragments of the *129/Sv-14qC3* locus comprising the following: (5′ tag) a 2.4-kb (primers: forward, 5′-AGCTTTAGGCATGCACTCAC-3′; reverse, 5′-GAGGCTGGTTGCA-CAAAGAC-3′) and a 2.8-kb (primers: forward, 5′-GGAAGGAT-GAGCTAGGACAG-3′; reverse, 5′-TCTGGAATCACTTTGTGGTCTC-3′) PCR-generated fragment of a transcriptionally inactive region 20 kb upstream of exon 1 of *dleu5*; (3′ tag) a 2.5 kb (primers: forward, 5′-CAGTCATCCATCGACAGCTG-3′; reverse, 5′-TATCAACACCAT-GCTCTTAAAC-3′) and a 2.3 kb (primers: forward, 5′-TCCACTGGCGTC-CACTGAAAG-3′; reverse, 5′-GAGCTGTGGTTTTAGATTATGC-3′) PCR-generated fragment downstream of the last exon of *Gucy1b2*. The linearized 5′ tag vector was electroporated into W9.5 embryonic stem (ES) cells derived from *129/SvEvTac*, and correctly targeted ES cell colonies were identified by Southern blot analysis after selection with ganciclovir and G418 (supplemental Figure 1-A1). The identified ES cells were electroporated with the linearized 3′ tag vector, and correctly targeted ES cell colonies were identified by Southern blot analysis after selection with ganciclovir and hygromycin (supplemental Figure 1-A2). ES clones with both targetings on the same chromosome were identified by Adeno-Cre (a gift from J. Kitajewsky, Columbia University, New York, NY) transduction and identification of eGFP-expressing ES cells by flow cytometry (supplemental Figure 2); correct deletion of the *loxP*-flanked *MDR* was verified in the corresponding cultures by Southern blot analysis (Figure 1C and supplemental Figure 1-A4). Chimeras were obtained after injection of the targeted ES clones into blastocysts derived from *C57BL/6* mice. From the

chimeras, we obtained mice with the *loxP*-flanked *CDR* allele in germline *CDR*^{fl/+}, as determined by Southern blot analysis. The chimeras were also crossed with *129/Sv^{CAGGS-Flp}* mice (The Jackson Laboratory) to generate a null allele without eGFP expression (supplemental Figure 1-A3). The obtained *CDR*^{+/-} mice were crossed to *C57BL/6* mice, and the resulting F1 generation was intercrossed to obtain *CDR*^{-/-} mice. Because *CDR* deficiency led to embryonic lethality, we interbred *CDR*^{+/-} with littermate wild-type mice to establish the experimental mice of the “constitutional” *CDR*^{+/-} knockout cohort, which were therefore of a *129/Sv-C57BL/6* mixed background. *CDR*^{fl/+} chimeras were bred with *C57BL/6* mice, and these mice were intercrossed with CD19-Cre mice for establishing the experimental mice of the conditional knockout cohort and were therefore of the *129/Sv-C57BL/6* mixed background. In vivo deletion of the *loxP*-flanked *CDR* allele was verified by Southern blot analysis of purified B cells derived from *CDR*^{fl/+}CD19-Cre mice (Figure 1C). Mice were housed and treated according to the guidelines of the Institute of Comparative Medicine at Columbia University (New York, NY).

Cell isolation, flow cytometry, and histology

Blood was withdrawn from the hearts of killed mice with a heparin-coated syringe and erythrocytes were subjected to 2 consecutive hypotonic lyses. Peritoneal cavity cells were isolated by flushing with 0.5% BSA in PBS. BM cells were flushed out of the tibia or femur using a syringe filled with PBS/BSA. Spleen cell suspensions were subjected to hypotonic lysis. The Abs and labels used for single-cell suspensions from spleen, peripheral blood (PB), peritoneal cavity, and BM have been described previously.²² Data were acquired on a FACSCalibur (BD Biosciences) using CellQuest software; data were analyzed using CellQuest Version 3.3 or FlowJo Version 9.3.2 software (TreeStar). Four-micrometer-thick, formalin-fixed, paraffin-embedded tissue sections were stained with H&E for morphologic analysis. Micrographs were taken with an Olympus BX41 bright-field microscope with the lens type UPlanFL. For a total magnification of 100×, the objective magnification was 10× and the numeric aperture was 0.30; for a total magnification of 200×, the objective magnification was 20× and the numeric aperture was 0.50. Photomicrographs were taken with a digital camera (Qcolor 3; Olympus) and Qcapture Version 2.90.1 software (Quantitative Imaging Corporation). The TIFF image format was converted to JPEG format using Adobe Photoshop Elements Version 2.0. Both flow cytometric and histological analyses were performed for all mice of the 15- to 18-month *CDR* cohort.

Event-free survival and statistical analysis

Tumor-watch studies were conducted on animals in a *129/Sv-C57BL/6* mixed background (ie, the first and second backcross generations). Mice were monitored for tumor incidence biweekly and were killed when visibly ill. Within the transgenic line, comparable numbers of age-matched wild-type littermates were controlled for possible differences in tumor incidence. Animals were monitored for up to 20 months. Statistical analysis was performed on the Prism Version 5 software program (GraphPad) using Kaplan-Meier cumulative survival and the log-rank (Mantel-Cox) test to determine whether differences were significant (Figure 5C). The χ^2 and/or the Fisher exact probability tests were used to compare B-cell lymphoproliferation incidence between the different genotypes of the *CDR* cohorts (Figures 4 and 5B) and to determine differences in the spectrum of lymphoproliferations among the *CDR*, *MDR*, and *miR-15a/16-1* cohorts (Figure 6). The Wilcoxon rank-sum test was used to determine differences in the CD5⁺ B-cell lymphoproliferations among the corresponding fractions (Figures 2 and 5A).

IgV gene sequence analysis

RNA was purified from PBMCs, splenic tissue, or lymph nodes from mice that were diagnosed with CD5⁺ or CD5⁻ B-cell lymphoproliferations after cell lysis with TRIzol reagent, and reverse transcribed into cDNA using (poly)dT oligonucleotides and Superscript II (Invitrogen). Rearranged VH sequences were amplified by PCR using forward primers that anneal to the framework region I of the mouse VH families, and reverse primers

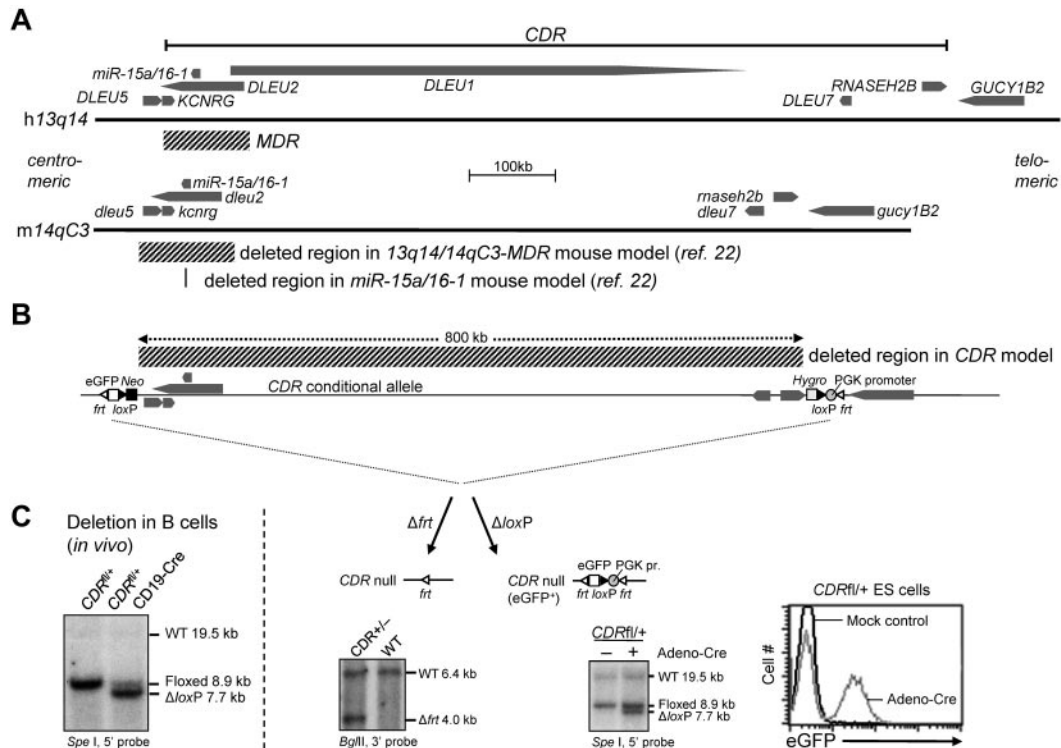


Figure 1. B-cell specific deletion of the *13q14*-*CDR* in mice. (A) Schematic representation of the human *13q14* and mouse *14qC3* locus. Genes and their 5'-3' orientation are indicated by thick arrows. The deleted regions in the *MDR* and *miR-15a/16-1* mouse models described previously²² are indicated. Because in humans, *KCNRG* is encoded within an intron of *DLEU2*, the former gene is considered part of the human *MDR*. In mice, and in contrast to what is found in humans, *dleu2*, in addition to *Kcnrg*, also overlaps with *dleu5* (exon 3 of *dleu5* is located in the last intron of *dleu2*), thus making *dleu5* part of the mouse *MDR*. (B) Schematic representation of the *CDR* targeting strategy (for details, see supplemental Figure 1-A1 to A4). Indicated are the expected fragments detected by Southern blot analysis after Flp-mediated recombination in mice, which generates an *CDR*-null allele, and after Adeno-Cre-mediated recombination in *CDR^{fl/+}* ES cells, which shows a $\Delta loxP$ fragment in addition to the targeted fragment, demonstrating the feasibility of deleting the 0.8-mb conditional *CDR* allele. Flow cytometric analysis of Adeno-Cre-treated *CDR^{fl/+}* ES cells shows that deletion of the *CDR* is accompanied by eGFP expression (for details, see supplemental Figures 1-2). (C) Deletion of the 0.8-mb *loxP*-flanked *CDR* allele in vivo. Southern blot analysis of *SpeI*-digested DNA from purified CD19⁺ B cells of *CDR^{fl/+}* CD19-Cre and *CDR^{fl/+}* mice. *CDR^{fl/+}* CD19-Cre mice show the WT allele and the allele after *loxP*-mediated deletion.

positioned in the JH1, JH2, JH3, and JH4 segments, as described previously.²² PCR products were gel-purified and sequenced directly (Genewiz). Sequences were compared with the ImMunoGeneTics database for sequence analysis (<http://www.imgt.org>). The MultiAlin sequence alignment algorithm²⁸ was used for hierarchical clustering of HCDR3 regions. IgV gene sequences are available upon request.

Results

Construction of mice deleting the *CDR* specifically in B cells and in germline

We have previously generated mice that have the *14qC3*-*MDR* deleted in the germline and also specifically in B cells using CD19-Cre mice²² (Figure 1A). The deleted region encompasses the *dleu2/miR-15a/16-1* cluster and the *Kcnrg* and *dleu5* genes that in mice, in contrast to humans, are located intronic of (*Kcnrg*) or overlap with (*dleu5*) *dleu2*. To investigate the consequences of deleting the entire *CDR*, which in addition comprises the protein-coding genes *dleu7* and *Rnaseh2b*, we generated a conditional mouse allele that on Cre- or Flpe-mediated deletion mimics the human *CDR* (Figure 1B). To generate a conditional *CDR* allele, we inserted 2 *loxP* and 2 *FRT* sites each by consecutive ES cell targetings into transcriptionally silent regions located 0.8 mb apart (Figure 1B; for details of the targeting strategy, see supplemental Figure 1-A1 and A2). The ES cell clone with the 5' site targeted is the same that was used in the generation of the conditional *MDR* allele²²; the 5' site is located approximately 20 kb centromeric to

dleu5. The 3' site is located between the *Rnaseh2b* and *Gucy1b2* genes, approximately 2 kb centromeric to the last exon of *Gucy1b2*. The placement of an eGFP mini gene in the centromeric (5' site), and a PGK promoter in the telomeric (3' site) targeting vectors that enable eGFP expression on Cre-mediated deletion of the *loxP*-flanked *CDR* (Figure 1B-C) allows screening for ES cell clones in which both targetings occurred on the same chromosome. Supplemental Figure 2A through D shows the general strategy (panel A), identification (panels B-C), and verification (panel D) of homologous recombination of the consecutive targetings. Correct homologous recombination and Cre-mediated deletion of the *loxP*-flanked region was confirmed by Southern blot analysis (Figure 1C and supplemental Figure 1-A1, A2, and A4). Mice harboring the *CDR^{loxP-FRT/+}* allele were bred with *Flp*-transgenic mice, and the correct deletion of the *FRT*-flanked region was confirmed by Southern blot analysis (Figure 1C and supplemental Figure 1-A3); these mice are further on designated as *CDR^{+/-}* mice. All animal experiments were approved by the institutional animal care and use committee review board of Columbia University.

Homozygous germline deletion of the *CDR* leads to embryonic lethality

Interbreeding *CDR^{+/-}* mice did not yield any *CDR^{-/-}* offspring. Of 214 mice born alive, 138 (64.5%) were *CDR^{+/-}* and 76 (35.5%) wild-type. Because *MDR^{-/-}* mice are born at Mendelian frequencies, this suggests that the additional 0.69 mb of DNA in the *CDR* encodes a genetic element or elements required for embryonic

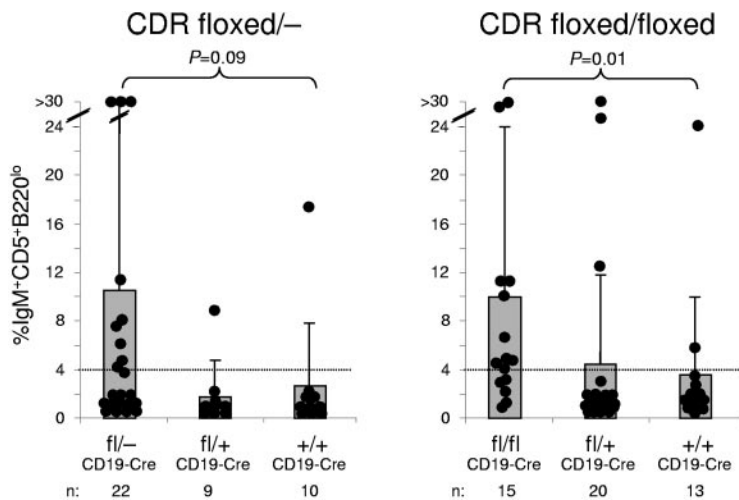


Figure 2. *CDR*-deleted mice develop CD5⁺ B-cell expansions in the PB. Percentages of CD5⁺B220^{lo} cells among mononuclear cells of mice from *CDR*^{fl/-}CD19-Cre and *CDR*^{fl/fl}CD19-Cre cohorts. *P* values (Wilcoxon rank-sum test) are indicated; the dotted line demarks the upper threshold for the normal range of CD5⁺B220^{lo} cells in a panel of 3- to 6-month-old wild-type mice determined by the average percentage ± 3σ; percentages above 4% are considered CD5⁺ lymphocytosis. Data are shown both as actual values (●) and as mean ± SD.

development, which is abrogated at an unknown time point by an unknown mechanism. Therefore, study of the role of the *CDR* in leukemogenesis requires a cell type-specific knockout approach.

Mice with *CDR* deletion specifically in B cells develop CLL

To determine the extent to which deletion of the *CDR* affects B-cell development and physiology, we generated mice that have the *CDR* in B cells specifically deleted by crossing *CDR*^{loxP-frt/+} mice with mice in which the Cre recombinase is under transcriptional control of the B cell-specific CD19 gene (CD19-Cre mice); these mice are further on referred to as *CDR*^{fl/+}CD19-Cre mice. Southern blot analysis of purified CD19⁺ B cells demonstrated the ability of the conditional *CDR* allele to recombine in vivo at an approximately 90% deletion efficiency (Figure 1C).

We generated cohorts of *CDR*^{fl/-}CD19-Cre and *CDR*^{fl/fl}CD19-Cre mice to achieve homozygous deletion of the *CDR* specifically in B cells, and the corresponding heterozygous and wild-type controls, *CDR*^{fl/+}CD19-Cre and CD19-Cre mice. Two- to 3-month-old mice with homozygous deletion of the *CDR* in B cells showed

normal percentages of B-cell subpopulations (supplemental Figure 3), and histologic analysis showed normal development of lymphoid organs (data not shown). These results suggest that homozygous deletion of the *CDR* does not impair B-cell development in young mice. In contrast, at approximately 12 months of age, *CDR*^{fl/-}CD19-Cre and *CDR*^{fl/fl}CD19-Cre mice began to develop CD5⁺B220^{lo} clonal lymphoproliferations in the PB (Figure 2), virtually all of which had the characteristics of CLL, BM and peripheral tissue involvement by CD5⁺B220^{lo} tumor cells (Figure 3A-B). The clonality of these lymphoproliferations was confirmed by PCR for rearranged IgV genes (supplemental Table 1). Clonal CD5⁺ lymphoproliferations occurring in the PB were IgM^{hi}IgD⁺ (Figure 3A), and infiltration of lymphoid and other organs was observed frequently (Figure 3B). In the spleen, the white pulp was enlarged as the result of an accumulation of small lymphocytes that showed histopathologic features of human CLL/small cell lymphocytic leukemia (Figure 3B top). Aggregates of small lymphocytes were also noted in the BM (Figure 3B middle), a finding consistent with the appearance of a B220⁺eGFP⁺ population in the BM by

Figure 3. *CDR*-deleted mice develop CLL. (A) Flow cytometry of PBMC (PB), splenic (Sp), or BM cells from a mouse presenting with CLL/small cell lymphocytic leukemia (SLL) and a wild-type (WT) mouse as control for CD5 and the B-cell marker B220 (top), IgM and IgD (middle), and eGFP and B220 (bottom). The CLL/SLL case shows a predominant CD5⁺B220^{lo} population in the spleen and PB that was IgM^{hi}IgD^{low} and eGFP⁺, demonstrating that the tumor clone is indeed derived from a *CDR*-deleted B cell. (B) Representative H&E-stained spleen, BM, and liver sections from *CDR*-deleted mice presenting with CLL/SLL (right) and an age-matched WT mouse (left). CLL/SLL section shows enlargement of the splenic white pulp by the expansion or accumulation of small B cells with architectural and morphologic features of CLL/SLL (top), aggregates of small lymphocytes in the BM (middle) and liver (bottom). Both flow cytometric and histological analysis were performed for all mice of the 15- to 18-month-old *CDR* cohort (for numbers of mice analyzed, see Figures 4 and 5; for details regarding micrographs, see "Cell isolation, flow cytometry, and histology").

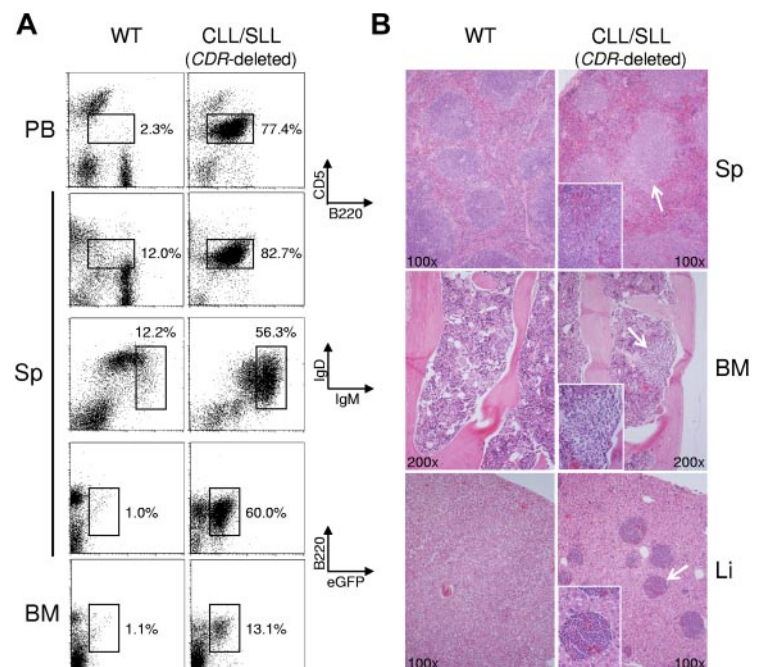
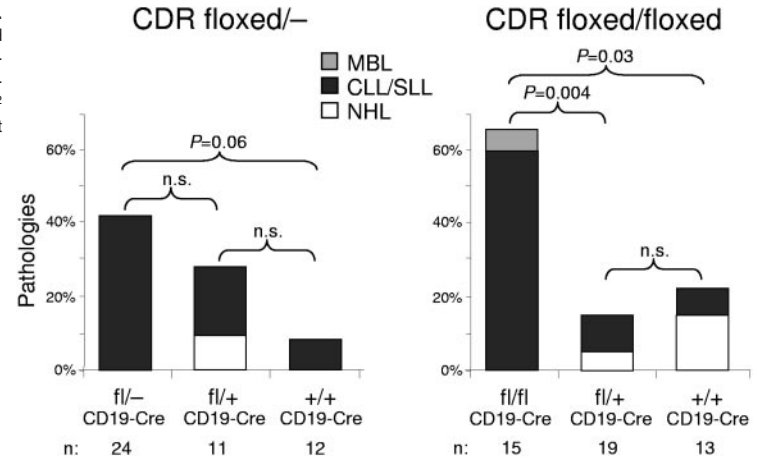


Figure 4. Mice with deletion of *CDR* develop lymphoproliferations. Percentages of B-lymphoid pathologies observed in 15- to 18-month-old mice of the *CDR^{fl/-}*-CD19-Cre and *CDR^{fl/fl}*-CD19-Cre cohorts. The percentages of MBL, CLL/small cell lymphocytic leukemia (SLL), and non-Hodgkin lymphoma (NHL) in each genotype are color coded. *P* values (χ^2 test of association) among the genotypes are indicated; n.s. indicates not significant.



flow cytometric analysis (Figure 3A bottom) and in the liver (Figure 3B bottom). In summary, the phenotype of the tumor cells and the histopathological features were consistent with CLL/small cell lymphocytic leukemia.

Mice with deletion of the *CDR* show a penetrance of lymphoproliferations similar to that of *MDR*-deleted mice

Forty-two percent of 15- to 18-month-old *CDR^{fl/-}*-CD19-Cre and 67% of *CDR^{fl/fl}*-CD19-Cre mice developed clonal lymphoproliferations (Figure 4). The higher penetrance of the phenotype in *CDR^{fl/fl}*-CD19-Cre compared with *CDR^{fl/-}*-CD19-Cre mice was not significant, likely because of the smaller number of mice analyzed in the former cohort. Overall, the frequency of lymphoproliferations in mice with *CDR* deletion in B cells was higher than that reported previously for *miR-15a/16-1* deletion (26% and 34% in *miR-15a/16-1^{-/-}* and *miR-15a/16-1^{fl/-}*-CD19-Cre mice, respectively)²² and in the same range as that of the *MDR* deletion (each 42% in the *MDR^{-/-}* and *MDR^{fl/-}*-CD19-Cre mice, respectively).²²

Mice with deletion of the *CDR* exhibit an indolent disease course but succumb to their disease faster than *MDR*-deleted mice

In agreement with the notion that heterozygous deletion of the chromosome 13q14 tumor-suppressor region is sufficient to promote lymphoproliferations, we observed previously that *MDR^{+/-}* mice, in contrast to wild-type mice, showed a trend toward developing clonal lymphoproliferations.²² We therefore established a cohort of *CDR^{+/-}* mice and wild-type littermates of sufficient size to permit statistical evaluation and analyzed 15- to 18-month-old mice for the occurrence of CD5⁺ lymphoproliferations in the PB, B-cell pathologies, and survival (Figure 5A-C). *CDR^{+/-}* mice

developed PB CD5⁺ lymphoproliferations more frequently than wild-type mice (Figure 5A) and also showed a trend toward harboring B-cell malignancies at an elevated frequency (Figure 5B; 25% vs 8% observed in wild-type mice). The event-free survival curves showed that *CDR^{+/-}* mice died sooner than their wild-type littermates (*P* = .0002; Figure 5C). Comparing survival of the *CDR* and *MDR* cohorts, 70% of *CDR^{+/-}* versus 45% of *MDR^{+/-}* mice had died at 20 months (supplemental Figure 4), suggesting that once *CDR^{+/-}* mice develop lymphoproliferations, they succumbed to their disease faster than *MDR^{+/-}* mice. In summary, *CDR^{+/-}* mice developed lymphoproliferations at a similar frequency compared with *MDR^{+/-}* mice²² (25% vs 24%, respectively), with a similar time of disease onset and a trend toward a more aggressive disease course compared with that observed in *MDR^{+/-}* mice.

Mice with deletion of the *CDR* display a different spectrum of lymphoproliferations compared with *MDR* and *miR-15a/16-1*-deleted mice

Fifteen- to 18-month-old *CDR^{fl/-}*-CD19-Cre and *CDR^{fl/fl}*-CD19-Cre mice developed clonal CD5⁺ lymphoproliferations, almost all of which represented CLL (Figure 4). This spectrum of lymphoproliferations differed significantly from those observed in the *miR-15a/16-1*- and *MDR*-deleted mice,²² which, in addition to CLL, also showed sizable frequencies of MBL and CD5⁻ non-Hodgkin lymphoma (Figure 6). These results suggest that a concomitant deletion of the genetic elements encoded in the chromosomal region telomeric to the *MDR*, while not elevating disease penetrance, does change the spectrum of B-cell malignancies. Because *CDR*-deleted mice show a diminished fraction of MBL, the presumed precursor of CLL, compared with *miR-15a/16-1* and

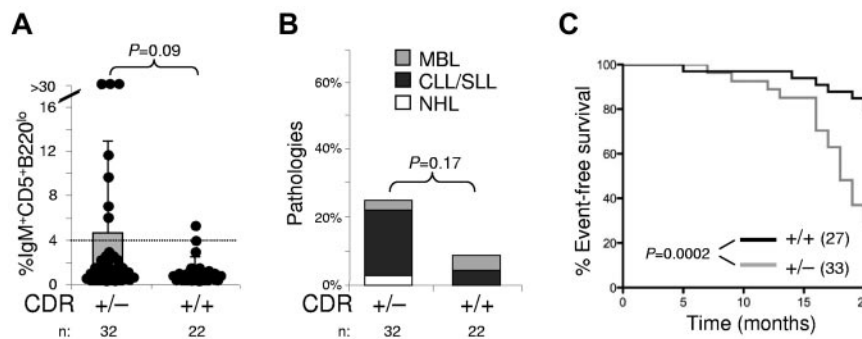


Figure 5. Mice with heterozygous deletion of the *CDR* develop lymphoproliferations and show an indolent disease course. (A) Percentages of CD5⁺B220^{lo} cells among mononuclear cells of mice from the *CDR^{+/-}* cohort. *P* values are indicated. For further details, see the legend to Figure 2. (B) Percentages of B-lymphoid pathologies observed in 15- to 18-month-old mice of the *CDR^{+/-}* cohort. For further details, see the legend to Figure 4. (C) Percentage of event-free survival in the *CDR^{+/-}* cohort. Mice were followed for 20 months. Events comprised illness or mice identified as moribund or sick (palpable tumor or visible ascites), which were killed. *P* values between the *CDR^{+/-}* and wild-type mice are indicated. The number of mice of each genotype is indicated in brackets. Mice shown in panels B and C correspond to different cohorts.

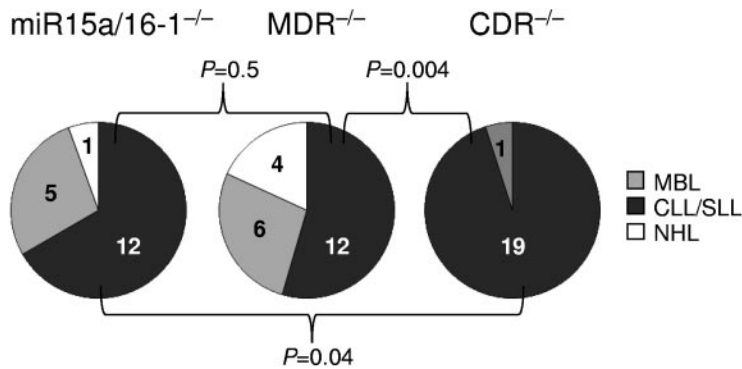


Figure 6. Spectrum of lymphoproliferations in mice with homozygous deletion of the *CDR*, *MDR*, and *miR-15a/16-1*. The fraction of CLL among the various types of B-lymphoproliferations in mice with homozygous deletion of the *CDR*, *MDR*, and *miR-15a/16-1* was statistically evaluated among the respective cohorts. *CDR*^{fl/fl} group: *CDR*^{fl/fl}CD19-Cre and *CDR*^{fl/fl}CD19-Cre mice; *MDR*^{fl/fl} group: *MDR*^{fl/fl} and *MDR*^{fl/fl}CD19-Cre mice²²; *miR-15a/16-1*^{fl/fl} group: *miR-15a/16-1*^{fl/fl} and *miR-15a/16-1*^{fl/fl}CD19-Cre mice.²²

MDR-deleted mice,²² this finding is suggestive of a faster transition of MBL to CLL or the bypass of a precursor stage in *CDR*-deleted mice. Together with the results from the event-free survival analysis (Figure 5C and supplemental Figure 4), this observation suggests that *CDR*-deleted mice develop more aggressive lymphoproliferations and succumb to their disease earlier than their *MDR* counterparts.

Stereotypic Ag receptors in CLL derived from different transgenic mice

Sequence analysis of PCR-amplified IgV genes from lymphoproliferations of homo- or heterozygous *CDR*-deleted mice from *CDR*^{fl/fl}CD19-Cre, *CDR*^{fl/fl}CD19-Cre, and *CDR*^{+/-} cohorts demonstrated that CD5⁺ tumors expressed unmutated IgV genes and CD5⁻ tumors somatically mutated IgV genes (supplemental Table 1). The same distribution was observed previously in the *MDR* and *miR-15a/16-1* cohorts.²²

CLL in humans is characterized by the expression of stereotypic Ag receptors; that is, the expression of structurally highly similar or identical BCR heavy chain complementary determining regions (HCDR3s) that arise from the rearrangement of the Ab gene segments (VDJ recombination) between unrelated individuals.²⁹⁻³² Comparing the altogether 27 amino acid sequences of the HCDR3 regions among the different lymphoproliferations derived from the *CDR* cohorts, we identified several clonal CD5⁺ B-cell proliferations that expressed stereotypic HCDR3 regions that are defined by displaying 80% or more homology at the protein level (Table 1). Comparison with 30 previously published HCDR3 regions from *MDR* and *miR-15a/16-1* cohorts²² revealed several distinct clusters of stereotypic HCDR3 regions (supplemental Table 2). *TCL1*-transgenic mice develop CLL similar to the *miR-15a/16-1*^{-/-}, *MDR*^{-/-}, and *CDR*-deleted mice.²⁶ Comparing all HCDR3 regions derived from MBL or CLL cases in our studies (46 from the present study and from Klein et al²²) and of the published *TCL1*-transgenic

Table 1. HCDR3 rearrangements of lymphoproliferations from *CDR*-deleted and wild-type mice

Animal	V _H	V _H	N	D _H	N	J _H	J _H	CDR3 length	Diagnosis
<i>CDR</i> ^{+/-} #40	V286	SR	GVE	IL	N	W	3	9	DLBCL
<i>CDR</i> ^{+/+} #51	V265	TR	R	GSSY		YYAMDY	4	13	CLL/SLL
<i>CDR</i> ^{+/-} #179-J4	V251	ARD	P	NWD	Y	YYAMDY	4	14	CLL/SLL
<i>CDR</i> ^{fl/fl} CD19-Cre #39	V054	AR	S	DYR	SQY	YYAMDY	4	15	CLL/SLL
<i>CDR</i> ^{fl/fl} CD19-Cre #47	V186	AR		IYDGY		YFDY	2	12	CLL/SLL
<i>CDR</i> ^{fl/fl} CD19-Cre #224	V122	ARD		DGY		YFDY	2	11	CLL/SLL
<i>CDR</i> ^{fl/fl} CD19-Cre #328	V332	AR	E	EA	G	YYAMDY	4	12	CLL/SLL
<i>CDR</i> ^{fl/fl} CD19-Cre #304-J1	V304		AS	HDYD		WYFDV	1	11	CLL/SLL
<i>CDR</i> ^{fl/fl} CD19-Cre #308-J2	V126	AR	G	YDYD		DYFDY	2	12	CLL/SLL
<i>CDR</i> ^{+/-} #117	V188	LR	EDK	YDG		FDY	2	11	DLBCL
<i>CDR</i> ^{fl/fl} CD19-Cre #184-J4	V027	VR		D	DYD	AMDY	4	10	CLL/SLL
<i>CDR</i> ^{+/-} #147	V054	AR	C	TTVVAT	KE	NAMDY	4	16	CLL/SLL
<i>CDR</i> ^{+/-} #67	V332	AR	R	DYGSSY		WYFDV	1	14	CLL/SLL
<i>CDR</i> ^{fl/fl} CD19-Cre #202	V332	AR	I	YGGSSY		WYFDV	1	14	CLL/SLL
<i>CDR</i> ^{fl/fl} CD19-Cre #27	V120	ARD		HYGSSY		AWFAY	3	14	CLL/SLL
<i>CDR</i> ^{fl/fl} CD19-Cre #178	V126	AR	DP	YYYGSS	L	YFDY	2	16	CLL/SLL
<i>CDR</i> ^{+/+} #114	V235	MRY		GNY		WYFDV	1	11	MBL
<i>CDR</i> ^{+/-} #181	V235	MRY		GNY		WYFDV	1	11	CLL/SLL
<i>CDR</i> ^{+/-} CD19-Cre #225	V235	MRY		SNY		WYFDV	1	11	CLL/SLL
<i>CDR</i> ^{fl/fl} CD19-Cre #184-J1	V163	AS		YGY		WYFDV	1	11	CLL/SLL
<i>CDR</i> ^{fl/fl} CD19-Cre #308-J1	V328	AR	PS	LPY		WYFDV	1	12	CLL/SLL
<i>CDR</i> ^{+/-} #174	V313	AR	GVY	DGY	PP	FDV	1	15	CLL/SLL
<i>CDR</i> ^{fl/fl} CD19-Cre #330	V286	AR	ERL	DGY	E	AWFAY	3	15	CLL/SLL
<i>CDR</i> ^{+/-} #179-J1	V190	AK	E	PYSNY	D	WYFDV	1	16	CLL/SLL
<i>CDR</i> ^{fl/fl} CD19-Cre #304-J2	V346	AR		DYSN		YDY	2	9	CLL/SLL
<i>CDR</i> ^{fl/fl} CD19-Cre #14	V563	A	G	NW		DFDY	2	8	CLL/SLL
<i>CDR</i> ^{+/+} CD19-Cre #30	V364	AR				WDFDV	1	7	CLL/SLL

The order of cases is according to the alignment obtained after hierarchical clustering of all HCDR3 sequences. Cases that showed ≥ 80% amino acid sequence homology in the CDR3 are grouped.

Table 2. Stereotypic HCDR3 rearrangements of lymphoproliferations from *CDR*, *MDR*, and *miR-15a/16-1*-deleted and *TCL1*-transgenic²⁶ mice

Animal	V _H	V _H	N	D _H	N	J _H	J _H	CDR3 length	Stereotype set
MDR ^{+/-} #175-PB	V261	AG	DR	YGY		WYFDV	1	12	I
TCL1_001	V261	AG		DRRGY		WYFDV	1	12	I
TCL1_002	V261	AG		DRTGY		WYFDV	1	12	I
CDR ^{fl} CD19-Cre #178	V126	AR	DP	YYYGSS	L	YFDY	2	16	II
MDR ^{fl} CD19-Cre #211	V126	AR		YYYGSSY		YFDY	2	13	II
TCL1_003	V4S1	AR		HYYGSSY		FDY	2	12	II
TCL1_004	V4S1	AR		HYYGSSY		FDV	1	12	II
TCL1_007	V332	AR		IYYGSSY		AMDY	4	14	III
TCL1_008	V1S61	AR		SYDGSYY		AMDY	4	14	III
CDR ^{+/+} #114	V235	MRY		GNY		WYFDV	1	11	IV
CDR ^{+/-} #181	V235	MRY		GNY		WYFDV	1	11	IV
MDR ^{-/-} #138	V153	MR		YGNV		WYFDV	1	11	IV
CDR ^{+/-} CD19-Cre #225	V235	MRY		SNV		WYFDV	1	11	IV
MDR ^{+/-} #27	V235	MR		YSNV		WYFDV	1	11	IV
TCL1_006	V153	MR		YSNV		WYFDV	1	11	IV
CDR ^{+/-} #67	V332	AR	R	DYGSSY		WYFDV	1	14	V
CDR ^{fl} CD19-Cre #202	V332	AR	I	YGGSSY		WYFDV	1	14	V
TCL1_010	V332	AR	I	YGGSSY		WYFDV	1	14	V
MDR ^{fl} -CD19-Cre #219	V128			YGGSSY		WYFDV	1	11	V
TCL1_005	V153	MR		YGGSSY		WYFDV	1	12	V
TCL1_009	V332	AR	R	YGGSS		WYFDV	1	13	V
miR ^{fl} -CD19-Cre #10	V328	A		IYYGNY		WYFDV	1	12	prov. VI
CDR ^{fl} -CD19-Cre #184-J1	V163	AS		YGY		WYFDV	1	11	prov. VI
MDR ^{fl} -CD19Cre #99	V328	AR		YYSNV		WYFDV	1	12	prov. VI
miR ^{fl} -CD19Cre #234	V328	AR	GEK	YSNV		WYFDV	1	14	prov. VI
CDR ^{fl} +CD19-Cre #47	V186	AR		IYDGY		YFDY	2	12	prov. VII
CDR ^{fl} -CD19-Cre #224	V122	ARD		DGY		YFDY	2	11	prov. VII
MDR ^{fl} -CD19-Cre #197	V227	A	SP	NWD		WYFDV	1	11	prov. VIII
MDR ^{+/+} CD19-Cre #212	V186	AR		NWD		WYFDV	1	10	prov. VIII

Order of cases is according to the alignment obtained after hierarchical clustering of all HCDR3 sequences. Cases that showed $\geq 80\%$ amino acid sequence homology in the CDR3 to the next neighbor/s are grouped. MDR and miR cases are derived from Klein et al,²² TCL1 cases from Yan et al.²⁶ Stereotype sets defined by Yan et al (sets I-V²⁶ and provisional [prov.] sets VI-VIII identified in the present work) are indicated in the right column.

study²⁶ (20 sequences), we observed that 44% (29 of 66) of the junctions can be assigned to 8 sets of highly similar HCDR3 regions among the sequence collection (Table 2). Several sequences of the *CDR*, *MDR*, or *miR-15a/16-1* cohorts could be assigned to 4 of 5 sets of stereotypic HCDR3 regions defined previously by Chiorazzi and colleagues.²⁶ Among the different transgenic mouse cohorts, 33% (2 of 6) of the sequences of the *miR-15a/16-1*, 53% (8 of 15) of the *MDR*, 36% (9 of 25) of the *CDR*, and 50% (10 of 20) of the *TCL1* cohorts could be assigned to the 8 sets of stereotypic HCDR3 regions. The higher fraction of stereotypic HCDR3 regions in the *TCL1* and *MDR* compared with any of the other cohorts did not reach statistical significance in a Fisher exact probability test. These observations suggest that the same Ags drive the expansion of the tumor cells in the *13q14* and *TCL1* transgenic mouse cohorts. Interestingly, in the clustering analysis of the HCDR3 regions of all 4 cohorts (Table 2), the *TCL1_005* and *TCL1_006* HCDR3 regions, that together comprised one stereotypic cluster in the analysis of Yan et al,²⁶ could be assigned to 2 different clusters (stereotype set IV and V in Table 2) characterized by the usage of different D genes (*DFL16.1* and *DSP2.x/DSP2.1*, respectively). This implies that expanding the set of HCDR3 sequences derived from the various CLL mouse models can lead to a more precise definition of stereotypic HCDR3 regions in mice. In summary, the occurrence of highly similar and identical (Table 2: *CDR*^{+/+}#114, *CDR*^{+/-}#181, and *MDR*^{-/-}#138; *CDR*^{+/-}CD19-Cre#225, *MDR*^{+/-}#27 and *TCL1_006*; *CDR*^{fl}CD19-Cre#202 and *TCL1_010*) HCDR3 regions between different transgenic mice that develop CLL provide additional evidence for a critical role for common Ags or auto-Ags in the clonal expansion of

the tumor cells. In accordance, the similarity of Abs of the stereotypic sets to murine Abs of known structure and Ag-binding specificities has been noted by Yan et al.²⁶

Discussion

Cre/loxP-mediated conditional deletion of a large chromosomal region in somatic cells

Large chromosomal deletions have been generated previously in mouse ES cells,³³⁻³⁵ and chromosomal translocations have been mimicked in somatic cells using Cre/loxP site-specific recombination.^{36,37} To our knowledge, the in vivo B cell-specific deletion of a 0.8-mb chromosomal region described here represents the largest conditional deletion that has been accomplished in somatic cells thus far. The deletion efficiency in B cells was high ($\sim 90\%$), possibly because of a good accessibility of the *14qC3* locus for the Cre recombinase. We have established a transgenic system in which the recombination-dependent juxtaposition of a promoter to a gene encoding a fluorescent marker signals Cre/loxP-mediated deletion and simultaneously permits the direct identification of ES cell clones when the 2 targetings occurred on the same chromosome (supplemental Figure 2). This system has the added advantage that such deleted cells can be detected and traced in vivo using fluorescence-based analysis (Figures 1 and 3), a feature that makes the cells amenable to functional and molecular analyses after FACS. The targeting approach described in the present work should be highly suitable for the analysis of chromosomal deletions that

occur with lower deletion efficiencies than that observed for the *CDR*, which would therefore be difficult to study without a fluorescent marker that unequivocally identifies the *Cre/loxP*-deleted cells.

Extent of *h13q14/m14qC3* deletions affects phenotype of lymphoproliferations and disease course

We demonstrated previously that mice with deletion of the *h13q14/m14qC3 MDR*, while developing the same spectrum of lymphoproliferations, show a higher penetrance of the phenotype and a more severe disease course compared with *miR-15a/16-1*-deleted mice.²² The present study found that mice with deletion of the *CDR* develop a different spectrum of lymphoproliferations compared with both *MDR*- and *miR-15a/16-1*-deleted mice,²² and suggests that *CDR*-deleted mice succumb to their disease earlier than *MDR*-deleted mice. However, both the time of disease onset and disease penetrance were similar to those of *MDR*-deleted mice.²² Because the *miR-15a/16-1*, *MDR*, and *CDR* cohorts were set up over a similar time period and housed in the same animal room, and because the different cohorts were analyzed over largely the same time span, we consider it unlikely that environmental or seasonal influences could account for the observed differences. We note that the similarity of the late disease onset (~ 1 year) and low penetrance (~ 20%-40%) of the *miR-15a/16-1*-, *MDR*-, and *CDR*-deleted mice suggests a role for additional genetic mutations^{7,8} and/or predisposing factors^{38,39} in the development of CLL in these mouse models mimicking the heterogeneous *13q14* deletions. It will be interesting to determine the nature of these factors.

The present study focused on *13q14* deletions affecting the *MDR* and the telomeric region of this tumor-suppressor locus. Subtypes of *13q14* deletions have been identified with loss of DNA centromeric to the *DLEU2/miR-15a/16-1* cluster, a fraction of which includes the *retinoblastoma (Rb1)* tumor-suppressor gene,¹⁶ and that have a less favorable prognosis.⁴⁰⁻⁴³ Inactivation of *miR-15a/16-1*, the expression of which is invariably ablated in all CLL with *13q14* aberrations, has functionally overlapping effects with *Rb1* deletion, because *miR-15a/16-1* down-regulates the expression levels of G₀-G₁/S-phase-promoting proteins that normally lead to Rb phosphorylation and result in cell-cycle entry. A concomitant deletion of both *miR-15a/16-1* and *Rb1* may accelerate the disease course.

These observations suggest that, whereas deletion of the *miR-15a/16-1* cluster is the critical mechanism in the pathogenesis of CLL with *13q14* aberrations, the additional loss of genetic elements encoded in the *13q14* tumor-suppressor locus can significantly influence the penetrance of the phenotype, the spectrum of the lymphoproliferations, and the severity of the disease course.

Narrowing down the critical genetic elements in the *13q14* tumor-suppressor locus

The results obtained from the investigation of the tumor-suppressor function of the *13q14* locus through *miR-15a/16-1*, *MDR*, and *CDR* conditional knockout mouse models collectively demonstrate that inactivation of the microRNA cluster *miR-15a/16-1* alone can cause lymphoproliferations, and that the concomitant deletion of other genetic elements located in the *MDR* and *CDR* leads to more aggressive phenotypes. The high conservation between the human *13q14* and murine *14qC3* loci with regard to both the identity of genes and the gene order (Figure 1A; *DLEU1* represents the only exception), along with a similar spectrum of diseases developing in both human and mouse, strongly imply that the *14qC3* mouse

models faithfully recapitulate the heterogeneous *13q14* deletions observed in humans.

h13q14/m14qC3 MDR

The genetic elements located in the *MDR* include *DLEU2*, which produces a long noncoding RNA and the protein-encoding genes *DLEU5* and *KCNRG*. *DLEU2* is the host gene of *miR-15a/16-1*, and its essential role in providing the primary transcript of these microRNAs is demonstrated by the complete ablation of *miR-15a/16-1* production on specific deletion of the *DLEU2/dleu2* promoter region⁴⁴ (and our own unpublished observations); this particular deletion that leaves the *miR-15a/16-1* gene cluster intact has been described to occur in vivo in several CLL cases.^{17,40,44} An unresolved issue is whether *DLEU2* has any additional roles, because experiments aimed at identifying an independent function for the *DLEU2* transcript, the sequence of which does not display homology to any other long noncoding RNA, have not yielded any insights.^{22,44} A further question regarding a potential function of *DLEU2* transcripts is whether the processed pseudogene *DLEU2L*, encoded on chromosomal region *1p22*, may compensate for the loss of *DLEU2* in CLL with *13q14* deletions. Likewise, it remains to be determined to what extent expression of the *miR-15b/16-2* cluster complements the biologic effects of *h13q14/m14qC3* deletions and, in turn, whether genetic mutations in this region exacerbate the pathogenesis of CLL with *h13q14/m14qC3* deletions. Whereas both *DLEU5* and *KCNRG* are considered to be located outside of the *MDR* in humans, these genes are deleted in a sizable fraction of CLL cases and therefore their functional inactivation may potentially contribute to the aggressiveness of the phenotype. The biologic function of *KCNRG* is only beginning to be understood⁴⁵; however, its low or absent expression in mature B-cell subpopulations (unpublished observations) would argue against its being a candidate tumor suppressor in CLL. *DLEU5* encodes a protein of unknown function. In the mouse, the *dleu5* gene overlaps with *dleu2*, and the genes are located in opposite transcriptional orientations (Figure 1A). In the human, the exons encoding the major form of the polyadenylated *DLEU2* transcript do not overlap with the *DLEU5* exons, although rare transcripts have been reported that use putative *DLEU2* downstream exons overlapping with the *DLEU5* gene.⁴⁶ Such alternative *DLEU2* transcripts were suggested to function as an antisense RNA for *DLEU5*,⁴⁶ invoking a regulatory function of the *DLEU2* gene for *DLEU5* mRNA expression. Future investigations will need to clarify the functional interaction of the *DLEU2* and *DLEU5* genes and their respective roles in B-cell physiology and neoplastic transformation.

h13q14/m14qC3 CDR

The observation that *CDR*-deleted mice show a diminished fraction of MBL compared with *MDR*-deleted mice suggests that the corresponding genomic region contains a genetic element the deletion of which either causes a faster transition of MBL to CLL or the bypassing of the CLL precursor stage in *CDR*-deleted mice. The known genes encoded in the region telomeric to the *MDR* are *RNASEH2B* and *DLEU7*. There are no confirmed microRNAs or other small noncoding RNAs in this region in humans (Basso et al⁴⁷ and K. Basso and R.D.-F., unpublished observations; miRBase Release 17) or mouse (miRBase Release 17). Whereas the function of *RNASEH2B* in B cells is unknown, *DLEU7* was recently suggested to play a role in the negative regulation of cell-cycle entry based on functional assays performed in nonlymphoid cells,²⁴

implying that *DLEU7* is a *13q14* candidate tumor-suppressor gene that may contribute to the severity of disease. It cannot be excluded that the *CDR* contains an as-yet-unidentified regulatory DNA element that may control or modify the expression of genes encoded in the *h13q14/m14qC3* locus. In addition, it remains to be determined how deletion of *DLEU1*, which is not conserved in the mouse genome, influences CLL pathogenesis.

In summary, the present study contributes to characterizing and redefining the critical genetic elements in the *h13q14/m14qC3* tumor-suppressor locus. Because *13q14* deletions in humans are usually heterogeneous, these findings provide a clear rationale for determining the leukemogenic role of the individual genetic elements affected by deletions of the *13q14* locus in addition to that of *miR-15a/16-1*.

Clusters of stereotypic Ag receptors among independent CLL mouse models

The striking similarities of Ab HCDR3 regions derived from tumor cases of different CLL mouse models underscores the validity of previously identified clusters of stereotypic Ag receptors in *TCL1*-transgenic mice²⁶ and identifies additional clusters (Table 2). These findings provide a solid rationale for defining clusters of stereotypic Ag receptors in CLL-prone mice, which may potentially lead to the identification of their cognate Ags in a way similar to what has been accomplished for human CLL Abs that have a common stereotypic rearrangement.⁴⁸⁻⁵⁰ Knowing the identity of these Ags would provide the basis for establishing suitable animal models aimed at studying the dynamics of Ag dependency in CLL pathogenesis *in vivo*.

Correlative data strongly suggest a role for extrinsic Ags or auto-Ags in human CLL development. The present observations that transgenic mice mimicking CLL-associated genetic alterations develop lymphoproliferations with stereotypic Ab receptors support this concept by providing functional evidence that genetic

aberrations disrupting the control of cell growth and survival and chronic Ag stimulation cooperate in the clonal expansion of CLL tumor cells.

Acknowledgments

The authors thank Thomas Ludwig for advice on the generation of the transgenic mice, Lauren Bertin for help with the IgV gene analysis, and Kristie Gordon and Chenhong Liu of the Herbert Irving Comprehensive Cancer Center Flow Cytometry Shared Resource for expert cell isolation.

Authorship

Contribution: M.L. cloned the targeting constructs, screened for homologous recombinants, organized the establishment of cohorts, and genotyped the mice; A.C. performed the IgV gene analysis, flow cytometric analysis of blood samples, and *in vitro* stimulation assays; H.T. performed flow cytometric analysis of lymphoid and tumor tissue and prepared tissue samples for histology; Q.S. oversaw the ES cell work and performed blastocyst injections; T.M. established and maintained the cohorts; G.B. performed the pathology analysis and revised the manuscript; R.D.-F. designed the research and cowrote the manuscript; and U.K. devised the targeting strategy, designed the research, analyzed the data, and cowrote the manuscript.

Conflict-of-interest disclosure: The authors declare no competing financial interests.

IgV gene sequences are available upon request.

Correspondence: Ulf Klein, Herbert Irving Comprehensive Cancer Center, 1130 St Nicholas Ave R312, New York, NY 10032; e-mail: uk30@columbia.edu.

References

- Chiorazzi N, Ferrarini M. B cell chronic lymphocytic leukemia: lessons learned from studies of the B cell antigen receptor. *Annu Rev Immunol*. 2003;21:841-894.
- Ghia P, Caligaris-Cappio F. The origin of B-cell chronic lymphocytic leukemia. *Semin Oncol*. 2006;33(2):150-156.
- Klein U, Dalla-Favera R. New insights into the pathogenesis of chronic lymphocytic leukemia. *Semin Cancer Biol*. 2010;20(6):377-383.
- Landgren O, Albitar M, Ma W, et al. B-cell clones as early markers for chronic lymphocytic leukemia. *N Engl J Med*. 2009;360(7):659-667.
- Rawstron AC, Bennett FL, O'Connor SJ, et al. Monoclonal B-cell lymphocytosis and chronic lymphocytic leukemia. *N Engl J Med*. 2008;359(6):575-583.
- Döhner H, Stilgenbauer S, Benner A, et al. Genomic aberrations and survival in chronic lymphocytic leukemia. *N Engl J Med*. 2000;343(26):1910-1916.
- Puente XS, Pinyol M, Quesada V, et al. Whole-genome sequencing identifies recurrent mutations in chronic lymphocytic leukaemia. *Nature*. 2011;475(7354):101-105.
- Fabbri G, Rasi S, Rossi D, et al. Analysis of the chronic lymphocytic leukemia coding genome: role of NOTCH1 mutational activation. *J Exp Med*. 2011;208(7):1389-1401.
- Kalachikov S, Miglizza A, Cayanis E, et al. Cloning and gene mapping of the chromosome 13q14 region deleted in chronic lymphocytic leukemia. *Genomics*. 1997;42(3):369-377.
- Bullrich F, Fujii H, Calin G, et al. Characterization of the 13q14 tumor suppressor locus in CLL: identification of ALT1, an alternative splice variant of the LBU2 gene. *Cancer Res*. 2001;61(18):6640-6648.
- Corcoran MM, Rasool O, Liu Y, et al. Detailed molecular delineation of 13q14.3 loss in B-cell chronic lymphocytic leukemia. *Blood*. 1998;91(4):1382-1390.
- Liu Y, Corcoran M, Rasool O, et al. Cloning of two candidate tumor suppressor genes within a 10 kb region on chromosome 13q14, frequently deleted in chronic lymphocytic leukemia. *Oncogene*. 1997;15(20):2463-2473.
- Miglizza A, Bosch F, Komatsu H, et al. Nucleotide sequence, transcription map, and mutation analysis of the 13q14 chromosomal region deleted in B-cell chronic lymphocytic leukemia. *Blood*. 2001;97(7):2098-2104.
- Rondeau G, Moreau I, Bezieau S, et al. Comprehensive analysis of a large genomic sequence at the putative B-cell chronic lymphocytic leukaemia (B-CLL) tumour suppressor gene locus. *Mutat Res*. 2001;458(3-4):55-70.
- Stilgenbauer S, Nickolenko J, Wilhelm J, et al. Expressed sequences as candidates for a novel tumor suppressor gene at band 13q14 in B-cell chronic lymphocytic leukemia and mantle cell lymphoma. *Oncogene*. 1998;16(14):1891-1897.
- Ouillet P, Erba H, Kujawski L, et al. Integrated genomic profiling of chronic lymphocytic leukemia identifies subtypes of deletion 13q14. *Cancer Res*. 2008;68(4):1012-1021.
- Gunnarsson R, Mansouri L, Isaksson A, et al. Array-based genomic screening at diagnosis and follow-up in chronic lymphocytic leukemia. *Haematologica*. 2011;96(8):1161-1169.
- Calin GA, Dumitru CD, Shimizu M, et al. Frequent deletions and down-regulation of micro-RNA genes miR15 and miR16 at 13q14 in chronic lymphocytic leukemia. *Proc Natl Acad Sci U S A*. 2002;99(24):15524-15529.
- Calin GA, Cimmino A, Fabbri M, et al. MiR-15a and miR-16-1 cluster functions in human leukemia. *Proc Natl Acad Sci U S A*. 2008;105(13):5166-5171.
- Raveche ES, Salerno E, Scaglione BJ, et al. Abnormal microRNA-16 locus with synteny to human 13q14 linked to CLL in NZB mice. *Blood*. 2007;109(12):5079-5086.
- Garzon R, Calin GA, Croce CM. MicroRNAs in Cancer. *Annu Rev Med*. 2009;60:167-179.
- Klein U, Lia M, Crespo M, et al. The DLEU2/miR-15a/16-1 cluster controls B cell proliferation and its deletion leads to chronic lymphocytic leukemia. *Cancer Cell*. 2010;17(1):28-40.
- Hammarsund M, Corcoran MM, Wilson W, et al. Characterization of a novel B-CLL candidate gene—DLEU7—located in the 13q14 tumor suppressor locus. *FEBS Lett*. 2004;556(1-3):75-80.
- Palamarchuk A, Efanov A, Nazaryan N, et al. 13q14 deletions in CLL involve cooperating tumor suppressors. *Blood*. 2010;115(19):3916-3922.
- Rice G, Patrick T, Parmar R, et al. Clinical and molecular phenotype of Aicardi-Goutieres syndrome. *Am J Hum Genet*. 2007;81(4):713-725.

26. Yan XJ, Albesiano E, Zanoni N, et al. B cell receptors in TCL1 transgenic mice resemble those of aggressive, treatment-resistant human chronic lymphocytic leukemia. *Proc Natl Acad Sci U S A*. 2006;103(31):11713-11718.
27. Klein U, Casola S, Cattoretti G, et al. Transcription factor IRF4 controls plasma cell differentiation and class-switch recombination. *Nat Immunol*. 2006;7(7):773-782.
28. Corpet F. Multiple sequence alignment with hierarchical clustering. *Nucleic Acids Res*. 1988;16(22):10881-10890.
29. Messmer BT, Albesiano E, Efremov DG, et al. Multiple distinct sets of stereotyped antigen receptors indicate a role for antigen in promoting chronic lymphocytic leukemia. *J Exp Med*. 2004;200(4):519-525.
30. Tobin G, Thunberg U, Karlsson K, et al. Subsets with restricted immunoglobulin gene rearrangement features indicate a role for antigen selection in the development of chronic lymphocytic leukemia. *Blood*. 2004;104(9):2879-2885.
31. Widhopf GF, 2nd, Rassenti LZ, Toy TL, et al. Chronic lymphocytic leukemia B cells of more than 1% of patients express virtually identical immunoglobulins. *Blood*. 2004;104(8):2499-2504.
32. Ghia P, Chiorazzi N, Stamatopoulos K. Microenvironmental influences in chronic lymphocytic leukaemia: the role of antigen stimulation. *J Intern Med*. 2008;264(6):549-562.
33. Lindsay EA, Botta A, Jurecic V, et al. Congenital heart disease in mice deficient for the DiGeorge syndrome region. *Nature*. 1999;401(6751):379-383.
34. Ramírez-Solis R, Liu P, Bradley A. Chromosome engineering in mice. *Nature*. 1995;378(6558):720-724.
35. Buch T, Rieux-Laucat F, Forster I, Rajewsky K. Failure of HY-specific thymocytes to escape negative selection by receptor editing. *Immunity*. 2002;16(5):707-718.
36. Buchholz F, Refaeli Y, Trumpp A, Bishop JM. Inducible chromosomal translocation of AML1 and ETO genes through Cre/loxP-mediated recombination in the mouse. *EMBO Rep*. 2000;1(2):133-139.
37. Collins EC, Pannell R, Simpson EM, Forster A, Rabbitts TH. Inter-chromosomal recombination of Mll and Af9 genes mediated by cre-loxP in mouse development. *EMBO Rep*. 2000;1(2):127-132.
38. Di Bernardo MC, Crowther-Swanepoel D, Broderick P, et al. A genome-wide association study identifies six susceptibility loci for chronic lymphocytic leukemia. *Nat Genet*. 2008;40(10):1204-1210.
39. Kikushige Y, Ishikawa F, Miyamoto T, et al. Self-renewing hematopoietic stem cell is the primary target in pathogenesis of human chronic lymphocytic leukemia. *Cancer Cell*. 2011;20(2):246-259.
40. Parker H, Rose-Zerilli MJ, Parker A, et al. 13q deletion anatomy and disease progression in patients with chronic lymphocytic leukemia. *Leukemia*. 2011;25(3):489-497.
41. Dal Bo M, Rossi FM, Rossi D, et al. 13q14 deletion size and number of deleted cells both influence prognosis in chronic lymphocytic leukemia. *Genes Chromosomes Cancer*. 2011;50(8):633-643.
42. Mian M, Rinaldi A, Mensah AA, et al. Del(13q14.3) length matters: an integrated analysis of genomic, fluorescence in situ hybridization and clinical data in 169 chronic lymphocytic leukaemia patients with 13q deletion alone or a normal karyotype [published online ahead of print June 13, 2011]. *Hematol Oncol*. doi:10.1002/hon.997.
43. Ouillette P, Collins R, Shakhani S, et al. The prognostic significance of various 13q14 deletions in chronic lymphocytic leukemia. *Clin Cancer Res*. 2011;17(21):6778-6790.
44. Lerner M, Harada M, Loven J, et al. DLEU2, frequently deleted in malignancy, functions as a critical host gene of the cell cycle inhibitory microRNAs miR-15a and miR-16-1. *Exp Cell Res*. 2009;315(17):2941-2952.
45. Biredinc A, Nohelty E, Marakhonov A, et al. Proapoptotic and antiproliferative activity of human KCNRG, a putative tumor suppressor in 13q14 region. *Tumour Biol*. 2010;31(1):33-45.
46. Corcoran MM, Hammarsund M, Zhu C, et al. DLEU2 encodes an antisense RNA for the putative bicistronic RFP2/LEU5 gene in humans and mouse. *Genes Chromosomes Cancer*. 2004;40(4):285-297.
47. Basso K, Sumazin P, Morozov P, et al. Identification of the human mature B cell miRNome. *Immunity*. 2009;30(5):744-752.
48. Chu CC, Catera R, Hatzki K, et al. Chronic lymphocytic leukemia antibodies with a common stereotypic rearrangement recognize nonmuscle myosin heavy chain IIA. *Blood*. 2008;112(13):5122-5129.
49. Catera R, Silverman GJ, Hatzki K, et al. Chronic lymphocytic leukemia cells recognize conserved epitopes associated with apoptosis and oxidation. *Mol Med*. 2008;14(11-12):665-674.
50. Lanemo Myhrinder A, Hellqvist E, Sidorova E, et al. A new perspective: molecular motifs on oxidized LDL, apoptotic cells, and bacteria are targets for chronic lymphocytic leukemia antibodies. *Blood*. 2008;111(7):3838-3848.